Engineering Structures 219 (2020) 110731

Contents lists available at ScienceDirect

Engineering Structures

journal homepage: www.elsevier.com/locate/engstruct

Behavior of reinforced concrete columns under biaxial shear forces based on ACI 318

Leonardo M. Massone*, Agustín Correa

Department of Civil Engineering, University of Chile, Chile

ARTICLE INFO

Keywords:
Columns
Biaxial
Design
Shear

ABSTRACT

Columns that are at the intersection of frames in two different directions are subjected to biaxial shear when lateral loads are simultaneously applied in two directions. Using the resultant shear and evaluating one-way shear strength along the direction of the resultant force, as most design codes do, is unconservative especially when significant shear co-exist about both axes. The conservatism of one-way shear strength in some expressions of ACI 318 (14) balances the not consideration of biaxial shear design in the code. However, the use of more refined or accurate expressions as in ACI 318 (19) makes the consideration of biaxial shear for design a need. Experimental data from the literature is used to compare ACI 318 expressions and validate the trilinear interaction diagram approach included in ACI 318 (19) for biaxial shear loading, showing that it is a simple and reliable method for design.

1. Introduction

Reinforced concrete columns prone to shear failure should be avoided in seismic design, due to their poor load-deformation performance [1] and fragile failure mode [2]. Short columns commonly fall within this category, given the high lateral load required to reach their flexural capacity. Although it is desirable to avoid such elements, short columns are often incorporated on purpose or as the result of a structural modification not considered in the original design. A clear type of unintentional short columns are the so-called captive columns, which have their effective length reduced when walls are incorporated in their lateral faces, restricting the movement in that direction [1]. Other structural elements that require special attention are the external corners columns in buildings, because during an earthquake they are subjected to biaxial loads, which might degrade the shear strength. The importance of the bidirectional response of frames in buildings during seismic events was recognized, after the Tokachi-Oki earthquake in 1968 and the San Fernando earthquake in 1971. More recently, researches have sought to understand the behavior of structural elements under multidirectional loads [3,4,5], but typically with an especial focus on slender columns exhibiting flexure-controlled response. Taking into consideration that flexure and shear strength in columns might degrade due to biaxial or multidirectional loads, actions in several directions require attention. In particular, the case of shear failure due to biaxial loading requires a review given that the effect of biaxial loading in flexure is nowadays commonly included in current versions of design codes, but not necessarily incorporated for shear design.

Umehara and Jirsa [4] examined the strength of short columns with square and rectangular sections under loading directions corresponding to the principal axes of the sections, as well as loading in diagonal directions. The results from 20 tests helped them to conclude that the shear capacity of short columns under skewed loading with respect to the principal axes could be estimated simply and accurately by using interaction curves. The curve that best represents the square column test results is an arch of a circle, and an ellipse for the case of the rectangular column tests. In the investigation by Joh and Shibata [6], nine specimens with a square cross-section and four specimens with a rectangular cross-section were subjected to biaxial lateral forces until they reached their shear failure. In their research, the interaction curve was normalized by the shear strength in the principal direction, yielding to Eq. (1). Pham and Li [5] presented an experimental and numerical investigation carried out on reinforced concrete columns with light transverse reinforcement with an emphasis on how varying the directions of seismic loading influences the failure mechanisms of the columns. Seven half-scale RC columns were tested subjected to an axial load and a cyclic lateral force under double-curvature bending. In this investigation, similar results were drawn, as with previous authors, validating the use of an interaction curve for design. All these results indicate that by normalizing the biaxial shear strength projected in each direction by the correspondent uniaxial shear strength, it is possible to

* Corresponding author.
E-mail address: lmassone@uchile.cl (L.M. Massone).

https://doi.org/10.1016/j.engstruct.2020.110731
Received 18 January 2019; Received in revised form 10 September 2019; Accepted 28 April 2020
Available online 22 June 2020

propose an interaction curve that represents square and rectangular columns; which can be expressed as,

$$(V_{dx}/V_{nx})^2 + (V_{dy}/V_{ny})^2 = 1 \quad (1)$$

where V_{nx}, V_{ny} are the shear strength values in the strong and weak directions, V_{dx}, V_{dy} are the components of strength in the diagonal direction when projecting to the strong and weak directions, such that the shear strength in the diagonal direction is calculated as $\sqrt{V_{dx}^2 + V_{dy}^2}$. This acknowledges that a rectangular column under biaxial shear loading cannot withstand simultaneous loads that are consistent with the uniaxial shear strength in each direction and the better representation of biaxial shear strength is an elliptical (circular for symmetrical square columns) interaction curve based on the uniaxial shear strength in each direction.

The vast majority of design codes do not include the effect of biaxial loading in the calculation of shear strength. Only the Japanese design code [7] has incorporated for many years a recommendation for the shear design of reinforced concrete columns when they are loaded biaxially. Lately, the ACI 318 code in its 2019 [8] version includes a section that treats biaxial loading with a similar approach as the Japanese code. The Japanese code for design incorporates the concept of the interaction curve by adding the consideration of Eq. (1) as a limit state in the commentary section of Chapter 9. It indicates that biaxial shear loading in column sections must lie within the interaction surface defined by Eq. (1), and also a structure importance factor (varying between 1 and 1.2) should be applied to the strength in the diagonal (V_d).

The current work, based on a collection of biaxial and uniaxial shear tests on columns from the literature, validates the use of the design code equations of ACI 318. First, by looking into the code equations that do not explicitly recognize the impact on shear strength of biaxial loading (ACI 318-14 [9]), and by looking into revised (and accurate) expressions in ACI 318 (19) [8] that recognize the impact of biaxial loading by incorporating a trilinear interaction curve in shear design.

2. Analysis of database

The database was collected from several works available in the literature [1, 3, 4, 5, 6, 10, 11, and 12]. Only the specimens that failed by shear and the load pattern were unidirectional or biaxial (also called diagonal) are used here. Thus, a total of 69 specimens were collected. Of the total tests, 53 specimens are columns with square cross-sections and 16 with rectangular cross-sections. The number of tests loaded in unidirectional and biaxial directions are 29 and 40, respectively. All specimens, except for three (all under unidirectional loading), were tested under lateral cyclic loads. The loading protocol for cyclic cases considered either one or three cycles per drift level with increasing drift levels in a unique direction in each test, either in one of the principal directions (uniaxial) or diagonally (biaxial). The loading system used in all the experimental programs is similar. The lower end of the specimen is fixed to a strong floor and the upper part is restricted to rotate, such that the tests represent a column under double curvature (both ends fixed).

Table 1 and Table 2 provide design parameters for square and rectangular specimens considered in this study; these design parameters fall within the ranges observed commonly in current design practice. The compressive strength of concrete, $f_c^{'}$, used in the tests ranged from 22 to 43 MPa, with an average of 30 MPa. The longitudinal steel ratio, ρ_w, ranged between 2.2% and 4.5%; and the transverse steel ratio, ρ_t, is between 0.09% and 0.51%. The shear span-to-depth ratio of the specimens is between 1.1 and 3.4 averaging a value of 1.5. The range of the axial load level, $N/(A_g \bullet f_c^{'})$, with A_g = cross-section and N = the axial load, for the compressed columns is between 0.15 and 0.54; and the range for the tensioned columns is between −0.09 and −0.11.

2.1. Interaction diagrams based on principal direction tests

A subset of the data in Tables 1 and 2, which includes only those columns for which specimen mechanical properties (geometry, longitudinal and transverse steel ratio and distribution, steel and concrete strength) are similar (ideally, they should be identical) for specimens subjected to uniaxial and biaxial loading, is used to validate an interaction surface such as that presented in Eq. (1). Limiting the dataset for model validation to these test specimens is required since the model assumes that strength measured in the principal directions (uniaxial loading) corresponds to the strength specimens loaded in the diagonal direction would have exhibited if loaded in the principal directions. In this case, a total of 61 specimens (49 square columns and 12 rectangular columns) are included out of 69. All experimental data in this section is presented normalizing the biaxial shear strength by the strength in both principal directions using measured uniaxial shear strength in the correspondent principal direction.

In Fig. 1, V_{bi}(x) and V_{bi}(y) represent the shear capacity of the biaxial test projected in “x” and “y” directions, respectively; and, V_{uni}(x) and V_{uni}(y) represent the shear capacity of the uniaxial tests. It is worth mentioning that V_{uni}(x) and V_{uni}(y) are identical for square columns. In Fig. 1a, the results are shown for square columns, and given the symmetry, the same data is shown in the “x” and “y” directions. It can be observed that there is a good correlation between the test results and the interaction curve (Eq. (1)), especially for cases with no axial load or compressive axial load. The dark triangles are columns with tensile axial load (N < 0), with failure close to its flexural capacity. In general, specimens with tensile axial load tend to show slightly higher biaxial shear capacity than specimens without axial load or compressive axial load, making the approach conservative (see Fig. 1a). Considering all square specimens, the mean value between the measured or experimental and the predicted strength (interaction curve – Eq. (1)) is $V_{exp}/V_n = 1.0$ with a standard deviation of 0.10 (Table 1).

From the database only three authors performed experiments with rectangular sections, which is shown in Fig. 1b, separated by test program. The plot shows a predictive curve using Eq. (1) and the values obtained from the tests. Again, the strength is normalized by the experimental shear strength obtained in each principal direction. The results obtained by Joh and Shibata [6] and Pham and Li [5] lie near the interaction curve; results obtained by Umehara and Jirsa [4] fall farther from the elliptical interaction curve. This may be due to the difference between the concrete compression strength for the unidirectional and biaxial tests in Umehara and Jirsa [4] experiments ($f_c^{'} = 35$ MPa for unidirectional tests and $f_c^{'} = 43$ MPa for biaxial tests), with a higher concrete compression strength in the biaxial tests. Ideally, for a direct comparison, all material properties should be identical, which is highly unlikely. In all other cases, the material properties used for unidirectional and biaxial tests present fewer differences. The results from the other two experimental programs provide a good correlation with the interaction curve. Considering all rectangular columns, the mean value between measured and predicted (interaction curve) strength is $V_{exp}/V_n = 1.03$ with a standard deviation of 0.10 (which reduces to 0.03 without Umehara and Jirsa tests). It should be noted that all rectangular specimens were conducted under considerable axial compression ($N/(A_g f_c^{'}) > 0.13$).

2.2. Interaction diagrams based on principal direction predictions by ACI 318 (2014) code

In this section, the biaxial experimental data is normalized by the uniaxial shear strength estimated with ACI 318 (2014) [9], as a way to see the accuracy of the code. The uniaxial ACI 318 (2014) equations used here are the simple and sophisticated equations for shear strength ($V_n = V_c + V_s$), which are separated in the concrete (V_c) and steel components ($V_s = \frac{A_v f_y d}{s}$, where d is the effective longitudinal

Table 1
Characteristics and strength estimates of square column specimens. (See below-mentioned references for further information.)

														Vn(Vnx, Vny) Eq. 1		ACI sophisticated		ACI simple		ACI 318-19	
Author	Specimen	Angle [°]	f'c [MPa]	bw [mm]	h [mm]	d [mm]	Vd/M	N/f'cAg	ρw	Av [mm²]	fyt [MPa]	s [mm]	Vexp [kN]	Vn [KN]	Vexp/Vn	Vn [KN]	Vexp/Vn	Vn [KN]	Vexp/Vn	Vn [KN]	Vexp/Vn
Maruyama et al. [3]	00-V-0-I Uni	0	35	305	305	219	0,48	0,00	0,034	57	469	65	258			171	1,51	157	1,65	174	1,48
	00-V-V-S Diag	45	35	305	305	219	0,48	0,00	0,034	57	469	65	264	258	1,02	171	1,54	157	1,69	174	1,51
	Monotonic	0	30	305	305	219	0,48	0,00	0,034	57	469	65	267			166	1,60	152	1,76	168	1,59
Ramirez et al. [10]	120C-U	0	31	305	305	219	0,48	0,19	0,034	57	448	65	280			184	1,53	174	1,61	229	1,22
Woodward et al. [1]	0-86-14-DM	45	41	305	305	219	0,48	0,00	0,034	57	503	65	245			183	1,34	168	1,45	188	1,30
	C-86-14-DM	45	36	305	305	219	0,48	0,16	0,034	57	503	65	302			196	1,54	192	1,58	246	1,23
Joh et al. [6]	SS-0-N0	0	23	300	300	222	0,49	0,00	0,034	57	307	63	215			131	1,64	115	1,87	130	1,66
	SS-0-N1	0	23	300	300	222	0,49	0,17	0,034	57	307	63	267			142	1,89	131	2,04	174	1,54
	SS-0-N2	0	23	300	300	222	0,49	0,33	0,034	57	307	63	266			176	1,51	146	1,83	194	1,37
	SS-45-N0	45	27	300	300	222	0,49	0,00	0,034	57	307	63	209	215	0,97	135	1,54	120	1,74	135	1,54
	SS-45-N1	45	24	300	300	222	0,49	0,17	0,034	57	307	63	260	267	0,97	143	1,82	132	1,97	175	1,49
	SS-45-N2	45	26	300	300	222	0,49	0,33	0,034	57	307	63	263	266	0,99	207	1,27	154	1,70	202	1,30
	SS-22.5-N0	22,5	22	300	300	222	0,49	0,00	0,034	57	307	63	211	215	0,98	130	1,62	115	1,84	129	1,64
	SS-22.5-N1	22,5	22	300	300	222	0,49	0,17	0,034	57	307	63	234	267	0,88	141	1,66	128	1,83	169	1,39
	SS-22.5-N2	22,5	25	300	300	222	0,49	0,33	0,034	57	307	63	265	266	1,00	189	1,40	150	1,76	199	1,34
Arakawa et al. [11]	0A0	0	32	180	180	132	0,59	0,00	0,045	25	249	64	101			45	2,25	36	2,83	44	2,27
	0A2	0	32	180	180	132	0,59	0,19	0,045	25	249	64	133			54	2,46	45	2,94	68	1,96
	0A4	0	34	180	180	132	0,59	0,35	0,045	25	249	64	148			97	1,52	56	2,64	70	2,10
	0A5	0	33	180	180	132	0,59	0,45	0,045	25	249	64	131			104	1,26	60	2,16	70	1,88
	2A0	22,5	32	180	180	132	0,59	0,00	0,045	25	249	64	93	101	0,93	45	2,08	36	2,62	44	2,10
	2A2	22,5	32	180	180	132	0,59	0,18	0,045	25	249	64	113	133	0,85	58	1,94	45	2,48	68	1,66
	2A4	22,5	31	180	180	132	0,59	0,38	0,045	25	249	64	132	148	0,89	93	1,41	54	2,43	68	1,95
	2A5	22,5	30	180	180	132	0,59	0,49	0,045	25	249	64	141	131	1,07	100	1,41	58	2,41	67	2,10
	4A0	45	34	180	180	132	0,59	0,00	0,045	25	249	64	96	101	0,95	46	2,11	36	2,64	45	2,11
	4A2	45	30	180	180	132	0,59	0,20	0,045	25	249	64	113	133	0,85	57	1,98	44	2,55	67	1,69
	4A4	45	32	180	180	132	0,59	0,37	0,045	25	249	64	132	148	0,89	94	1,41	55	2,43	68	1,94
	4A5	45	31	180	180	132	0,59	0,48	0,045	25	249	64	128	131	0,98	100	1,28	59	2,19	67	1,90

														Vn(Vnx, Vny) Eq. 1		ACI sophisticated		ACI simple		ACI 318-19	
Author	Specimen	Angle [°]	f'c [MPa]	bw [mm]	h [mm]	d [mm]	Vd/M	N/f'cAg	ρw	Av [mm²]	fyt [MPa]	s [mm]	Vexp [kN]	Vn [KN]	Vexp/Vn	Vn [KN]	Vexp/Vn	Vn [KN]	Vexp/Vn	Vn [KN]	Vexp/Vn
Mizoguchi et al. [12]	0V04+	0	26	180	180	132	0,59	0,44	0,045	38	273	41	137			108	1,27	71	1,91	84	1,63
	0V04-	0	26	180	180	132	0,59	0,00	0,045	38	273	41	95			63	1,50	54	1,76	62	1,53
	0V15+	0	26	180	180	132	0,59	0,57	0,045	38	273	41	139			113	1,23	75	1,85	83	1,67
	0V15-	0	26	180	180	132	0,59	-0,11	0,045	38	273	41	72			36	1,97	36	1,97	50	1,43
	0VA04+	0	27	180	180	132	0,59	0,44	0,045	38	273	41	133			108	1,23	72	1,86	84	1,58
	0VA04-	0	27	180	180	132	0,59	0,00	0,045	38	273	41	83			64	1,31	54	1,53	62	1,34
	0VA15+	0	27	180	180	132	0,59	0,54	0,045	38	273	41	136			116	1,17	77	1,77	85	1,60
	0VA15-	0	27	180	180	132	0,59	-0,11	0,045	38	273	41	68			36	1,88	36	1,88	51	1,34
	2V04+	22,5	31	180	180	132	0,59	0,39	0,045	38	273	41	142	137	1,04	113	1,25	74	1,91	88	1,61
	2V04-	22,5	31	180	180	132	0,59	0,00	0,045	38	273	41	94	95	0,99	65	1,46	56	1,70	64	1,47
	2VA04+	22,5	31	180	180	132	0,59	0,38	0,045	38	273	41	140	133	1,05	114	1,23	75	1,88	88	1,59
	2VA04-	22,5	31	180	180	132	0,59	0,00	0,045	38	273	41	94	83	1,14	65	1,45	56	1,69	64	1,47
	4V04+	45	29	180	180	132	0,59	0,40	0,045	38	273	41	133	137	0,97	112	1,19	74	1,80	87	1,53
	4V04-	45	29	180	180	132	0,59	0,00	0,045	38	273	41	96	95	1,01	65	1,49	55	1,74	64	1,50
	4V15+	45	29	180	180	132	0,59	0,52	0,045	38	273	41	130	139	0,93	118	1,10	77	1,68	86	1,51
	4V15-	45	29	180	180	132	0,59	-0,10	0,045	38	273	41	79	72	1,10	36	2,16	36	2,16	52	1,53
	4VA04+	45	29	180	180	132	0,59	0,40	0,045	38	273	41	145	133	1,09	112	1,30	73	1,97	87	1,67
	4VA04-	45	29	180	180	132	0,59	0,00	0,045	38	273	41	100	83	1,20	64	1,55	55	1,81	64	1,57
	4VA15+	45	30	180	180	132	0,59	0,50	0,045	38	273	41	143	136	1,05	119	1,20	78	1,83	87	1,65
	4VA15-	45	30	180	180	132	0,59	-0,10	0,045	38	273	41	89	68	1,30	37	2,44	37	2,44	52	1,71
Pham et al. [5]	S.C-2.4-0.20	0	23	350	350	255	0,30	0,20	0,028	57	393	125	219			136	1,61	141	1,55	199	1,10
	S.C-1.7-0.20	0	28	350	350	255	0,43	0,20	0,028	57	393	125	294			160	1,83	156	1,88	222	1,33
	S2.4-30	30	31	350	350	255	0,30	0,20	0,028	57	511	125	226	219	1,03	169	1,34	182	1,24	254	0,89
	S2.4-45	45	29	350	350	255	0,30	0,20	0,028	57	511	125	226	219	1,03	164	1,38	176	1,29	244	0,93
	S1.7-30	30	30	350	350	255	0,43	0,20	0,028	57	511	125	260	294	0,88	194	1,34	178	1,46	248	1,05
	S1.7-45	45	29	350	350	255	0,43	0,20	0,028	57	511	125	284	294	0,97	182	1,56	176	1,62	244	1,16

	Eq. 1 Vexp/Vn	ACI sophisticated Vexp/Vn	ACI simple Vexp/Vn	ACI 318-19 Vexp/Vn
Avg	**1,00**	**1,57**	**1,94**	**1,56**
SD	**0,10**	**0,33**	**0,39**	**0,30**
Max	**1,30**	**2,46**	**2,94**	**2,27**
Min	**0,85**	**1,10**	**1,24**	**0,89**

Table 2
Characteristics and strength estimates of rectangular column specimens.

Author	Specimen	f'c [MPa]	bw [mm]	h [mm]	d [mm]	Vd/M	N/f'cAg	ρw	Av [mm²]	fyt [MPa]	s [mm]	Angle [°]	Vexp	Vn(Vnx, Vny) Eq. 1: Vn [kN]	Vn(Vnx, Vny) Eq. 1: Vexp/Vn	ACI sophisticated: Vnx [kN]	ACI sophisticated: Vny [kN]	ACI sophisticated: Vdiag [kN]	ACI sophisticated: Vexp/Vn	ACI simple: Vnx [kN]	ACI simple: Vny [kN]	ACI simple: Vdiag [kN]	ACI simple: Vexp/Vn
Joh et al. [6]	SR-0-N1	24	225	400	302	0,66	0,17	0,033	57	307	71	0	263			176		176	1,49	146		**146**	1,80
	SR-90-N1	25	400	225	162	0,36	0,17	0,035	85	307	71	0	224			132		132	1,71	130		**130**	1,72
	SR-30-N1	25	225	400	302	0,66	0,17	0,033	57	307	71	30	249	251	0,99	184	132	165	1,51	149	131	**144**	1,74
	SR-60-N1	26	225	400	302	0,66	0,17	0,033	57	307	71	60	217	232	0,93	202	134	144	1,50	151	133	**137**	1,58
Umehara et al. [4]	OUS	40	229	406	284	0,63	0,00	0,044	57	414	89	0	294			171		171	1,72	145		**145**	2,03
	OUW	40	406	229	188	0,41	0,00	0,037	113	414	89	0	254			196		196	1,29	181		**181**	1,40
	CMS	42	229	406	284	0,63	0,14	0,044	57	414	89	0	383			204		204	1,87	176		**176**	2,18
	CUS	35	229	406	284	0,63	0,16	0,044	57	414	89	0	329			211		211	1,56	167		**167**	1,97
	CUW	35	406	229	188	0,41	0,16	0,037	113	414	89	0	267			204		204	1,31	207		**207**	1,29
	2CUS	42	229	406	284	0,63	0,27	0,044	57	414	89	0	405			329		329	1,23	205		**205**	1,97
	CDS30	43	229	406	284	0,63	0,13	0,044	57	414	89	30	356	310	1,15	210	211	210	1,69	177	218	**185**	1,93
	CDW30	42	229	406	284	0,63	0,14	0,044	57	414	89	60	329	279	1,18	217	211	213	1,55	176	217	**204**	1,61
Pham et al. [5]	R.C-1.7-0.35-S	27	250	490	379	0,45	0,35	0,024	57	393	125	0	346			225		225	1,54	208		**208**	1,66
	R.C-1.7-30	31	250	490	379	0,45	0,35	0,024	57	511	125	30	254	263	0,96	403	212	230	1,10	249	174	**184**	1,38
	R.C-1.7-45	30	250	490	379	0,45	0,35	0,024	57	511	125	45	221	221	1,00	391	171	187	1,18	242	167	**177**	1,25
	R.C-1.7-60	29	250	490	379	0,45	0,35	0,024	57	511	125	60	190	194	0,98	384	156	171	1,11	239	163	**173**	1,10
														Avg	1,03				1,46				1,66
														SD	0,10				0,23				0,31
														Max	1,18				1,87				2,18
														Min	0,93				1,10				1,10

reinforcement distance, A_v is the stirrups cross-sectional area, f_y is the steel yield stress, and s is the stirrups spacing). The simple and sophisticated equations differ in the number of variables considered for the concrete shear strength component (V_c).

(a) ACI 318 (2014) – simple concrete shear strength equation

The simple equation for the shear strength of concrete, in this case, is defined as,

$$V_c = \begin{cases} 0.17\left(1 + \frac{N}{14A_g}\right)\sqrt{f_c^{'}}b_w d, & if\ N > 0 \\ 0.17\left(1 + \frac{0.29N}{A_g}\right)\sqrt{f_c^{'}}b_w d, & if\ N < 0 \end{cases} \text{(SI units)} \quad (2)$$

where b_w is the column width.

Analogous to Fig. 1, Fig. 2 presents a normalized biaxial experimental data (along with uniaxial tests in both axes) for square columns, but in this case, the values of the tests are normalized with the shear strength in the principal axis calculated with the ACI 318 (2014) code equation (Eq. (2)) using the actual material properties. In this case, since the columns are symmetric (identical strength in both directions), the strength in any direction would be the strength in the principal direction. That is, according to Eq. (1), $(V_{dx}/V_{nx})^2 + (V_{dy}/V_{ny})^2 = (V_{dx}/V_n)^2 + (V_{dy}/V_n)^2 = 1$, such that, $(V_{dx})^2 + (V_{dy})^2 = (V_n)^2$, which indicates that the diagonal strength is equal to the strength in the principal directions. Similar to the previous case, the data is also separated by the level of axial load given the better accuracy observed in Fig. 1a for specimens with zero or compressive axial loads. Besides, the ACI 318 (2014) code equations also depend on the axial load. In this case, along both axes (same data), there is experimental data since the uniaxial prediction by ACI 318 is not necessarily identical to the experimental value.

As can be seen in Fig. 2, there are no test values below the biaxial strength prediction (interaction curve), which means that if the interaction curve is used to estimate the biaxial strength (and the uniaxial strength by ACI 318-14), it is conservative. The closest value to the interaction curve shown in the figure is $V_{exp}/V_n = 1.24$ (Table 1), but if only unidirectional strength estimation (without the interaction curve) is considered (dotted red lines), there is one case below 1.0 in both directions. When considering all test specimens, the mean value of the measured compared with the predicted strength (interaction curve) value is $V_{exp}/V_n = 1.94$ with a standard deviation (SD) of 0.39 (Table 1), with similar results when the data is separated by the axial load (tension, compression and no axial load). This indicates that the level of the axial load does not differentiate much the accuracy of the model.

On the other hand, the red dotted lines show the zone where the specimens with a traditional uniaxial design are unconservative. In this case (ACI 318 simple expression), only one specimen would fail before reaching the required capacity (no strength reduction factors are considered) for biaxial loading. That is, if the strength were estimated without the consideration of biaxial loading, as it is traditionally done by most design approaches, including the ACI 318 (2014), the design would not be conservative just for one specimen.

(b) ACI 318 (2014) – sophisticated concrete shear strength equation

A more sophisticated or refined expression is considered for the concrete component of shear strength in square columns. In the case of columns under compressive forces, Eq. (3) can be used as,

$$V_c = min\begin{Bmatrix} \left(0.16\lambda\sqrt{f_c^{'}} + 17\rho_w\frac{V_u d}{M_n}\right)b_w d \\ 0.29\lambda\sqrt{f_c^{'}}b_w d\sqrt{1 + \frac{0.29N_u}{A_g}} \end{Bmatrix}\text{(SI units)} \quad (3)$$

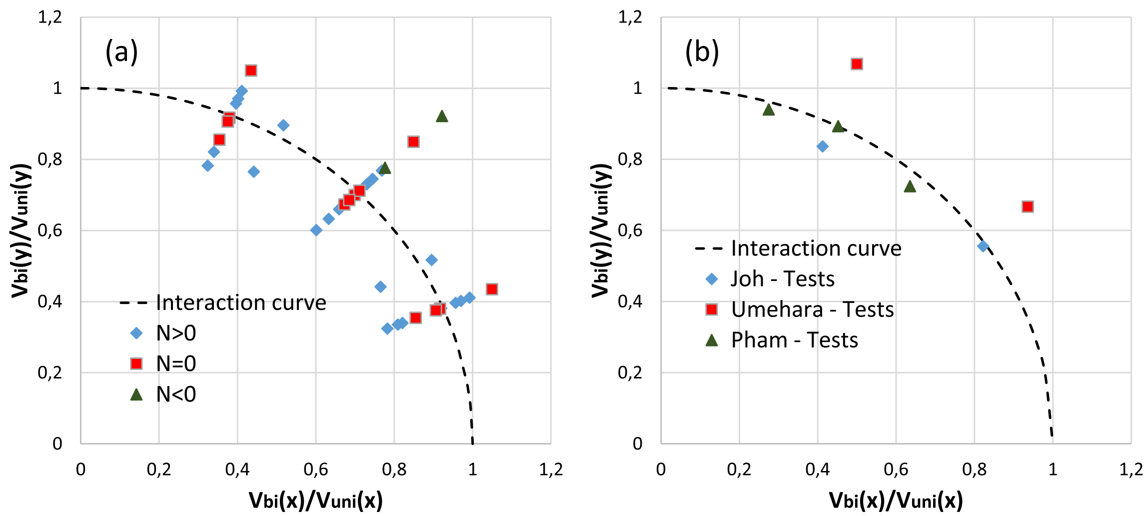

Fig. 1. Normalized shear strength versus direction of loading for – (a) square and (b) rectangular columns.

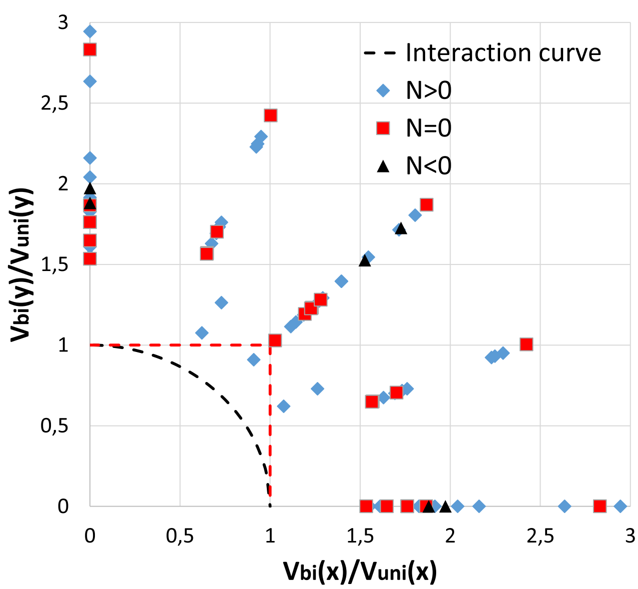

Fig. 2. Normalized shear strength versus direction of loading for square columns using ACI 318 (14) simple expressions.

where $M_n = M_u - N_u\left(\frac{4h-d}{8}\right)$; V_u, M_u, N_u is the factored design shear, moment and axial force, respectively; ρ_w is the steel longitudinal reinforcement ratio, h is the length of the column section and λ is a factor for lightweight concrete.

Thus, Fig. 2 is modified into Fig. 3a resulting in shear estimates less conservative, lowering the average from V_{exp}/V_n= 1.94 to 1.57 (Table 1) for square columns. In this case, more cases (increasing from 1 to 7 cases when the sophisticated equation is used instead of the simple equation) fall within the unconservative zone (red lines) when no biaxial design is considered, which are the specimens loaded in 45°.

Fig. 3b, similar to Fig. 3a, presents the normalized experimental data for rectangular columns considering both expressions from ACI 318 (2014). In this case, since the columns are nonsymmetrical (different strength in each direction), the strength in the loading direction is estimated according to Eq. (1), such that, the strength in the diagonal direction is $\sqrt{(V_{dx})^2 + (V_{dy})^2}$ and the relationship between V_{dx} and V_{dy} is $\tan\theta = V_{nx}/V_{ny}$, where θ is the loading angle (measured from the y-axis). As can be seen, all the points are over the interaction curve, being the closest at $V_{exp}/V_n = 1.10$, for the simple expression (Table 2). This means that for rectangular columns the simple expression is also conservative if the biaxial effect (interaction curve) is being considered. In this case, 2 columns, if analyzed without considering the interaction diagram would be unsafe since they are within the zone $V_{exp}/V_n < 1$, however, those specimens present detailing that is not ACI 318 compliant (less confinement). Such a number of specimens increases from 2 to 3 when the more sophisticated equation of ACI 318 (2014) is considered.

2.3. Alternative biaxial strength estimation – mechanical model

This methodology is based on a concept used by Woodward and Jirsa [1], which consists of applying directly the strength equations given by ACI 318, or other design codes, for uniaxial loading, but on a column whose cross-section is rotated to represent a diagonal or biaxial loading. The specimen CDS30 [4] (Fig. 4a) with a rectangular section and an axial load level of $N/f_c^{'}A_g = 0.14$ is considered as an example, where the diagonal load was applied with an inclination of 30° with respect to the strong axis. The first step is to find the location of the neutral axis of the element (Fig. 4b), where the column is rotated. In this case, the ultimate condition is imposed in flexure such that the most compressed fiber reaches a compressive strain of 0.003. The equilibrium approach recommended by ACI 318 (14) was used for the analysis. Using this information, d' is calculated, which corresponds to the distance from the most extreme fiber in compression to the centroid of the bars in tension in the rotated position. The contribution made by the concrete for the simple ACI 318 (14) equation is of the type $V_c = \alpha\sqrt{f_c^{'}}b_w d$, and as pointed out by Woodward and Jirsa, the term $b_w d$ can be replaced by the shaded area limited by d' (Fig. 4b), and thus determine the area of concrete that contributes to shear in the case of diagonal loading. For this example, the contribution of the shear reinforcement, considering that the stirrups work in the loading direction of the element (Fig. 4c), is given by $V_s = A_b f_y(2\cos30° + \sin30°)d'/s$, where A_b corresponds to the cross-sectional area of one of the stirrup legs.

Fig. 5 shows the results for square columns based on the mechanical approach and the ACI 318 (14) simple shear strength equation. The distribution of points closely resembles Fig. 2 (also normalized by the simple expression of ACI 318-14), including the distribution by axial load level. It is observed that the relation $V_{exp}/V_n = 1.92$ is slightly lower than in the case of Fig. 2, where a value of 1.94 is obtained, with similar scatter.

It should be noted that this methodology requires several calculations, since both the concrete and steel components must be estimated for each loading angle. On the other hand, the results also indicate that the strength estimates from this approach are very similar to the estimation in two orthogonal directions that account for biaxial design.

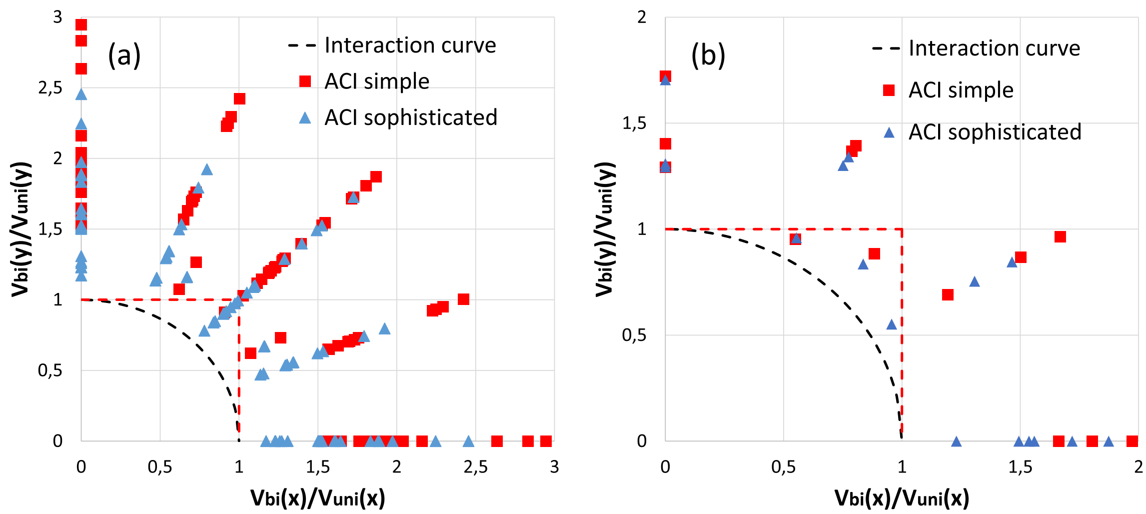

Fig. 3. Normalized shear strength versus direction of loading using ACI 318 (14) simple and sophisticated expressions for - (a) square and (b) rectangular columns.

2.4. Interaction diagrams based on principal direction predictions by ACI 318 (2019) code

ACI 318 (2019) [8] proposed a simplification of the shear equations and condensed them into new expressions, with better correlation when compared with test results [13], which at the same time implies less conservatism. The new expressions differentiate between elements that comply or not with the minimum shear reinforcement requirement. In under-reinforced cases in shear, a coefficient that includes size effect is incorporated. The experimental database considers only columns that comply with the minimum shear reinforcement requirement, such that only the consistent set of expression is used here to determine the shear strength of concrete (V_c), defined in Eq. (4) as,

$$V_c = Either\ of \begin{Bmatrix} \left(0.17\lambda\sqrt{f_c'} + \frac{N_u}{6A_g}\right)b_w d \\ \left(0.66\lambda(\rho_w)^{1/3}\sqrt{f_c'} + \frac{N_u}{6A_g}\right)b_w d \end{Bmatrix} (\text{SI units}) \tag{4}$$

where $0 \le V_c \le 0.42\lambda\sqrt{f_c'}b_w d$, and $\frac{N_u}{6A_g} \le 0.05f_c'$.

This new formulation is evaluated only for square columns. The formulation results in a more precise estimation of shear strength (Fig. 6) than the simple ACI 318 (14) expression, and similar to the sophisticated expressions with an overall average of V_{exp}/V_n= 1.56. Test results indicate that the circular interaction diagram can conservatively predict the shear capacity of columns under biaxial loading in most cases. Few cases fall within the unconservative zone when the biaxial design with the circular interaction curve is not considered (normalized strength below 1 in each direction), which are the specimens loaded

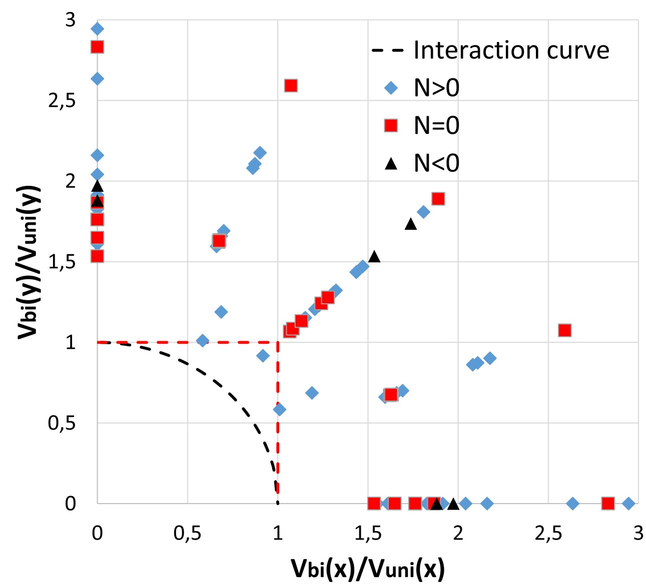

Fig. 5. Normalized mechanical shear strength versus direction of loading for square columns using ACI 318 (14) simple expressions.

between 30° and 60°. Thus, if no interaction diagram is used, that is, only uniaxial strength consideration is used for design, the strength might be underestimated by as much as 41% (45° loading with required capacity as $V_{bi} = 1/\cos(45°)V_{uni} = \sqrt{2}V_{uni}$) if we consider a square

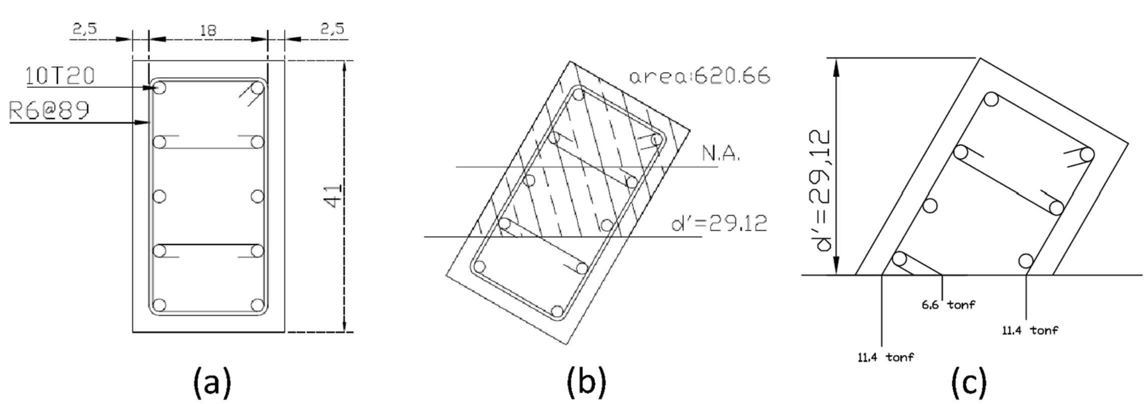

Fig. 4. (a) Specimen CDS30 [4] (dimensions in cm), (b) rotated column in 30° for biaxial loading, and (c) stirrups and ties contribution for biaxial loading.

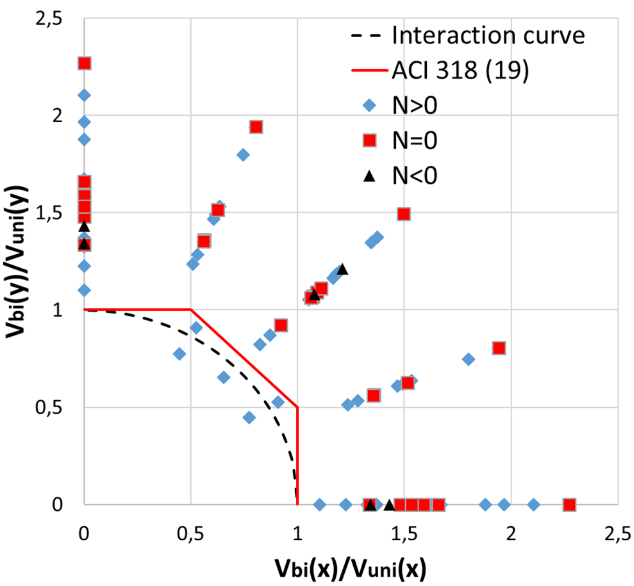

Fig. 6. Normalized shear strength versus direction of loading for square columns using ACI 318 (19) expressions and trilinear interaction curve.

(symmetric) column. The improved accuracy of the current approach of shear strength estimation in ACI 318 (19) implies that taking into account biaxial loading in design is now a more relevant consideration.

Regarding safety design, the level of error by not taking into account biaxial design is addressed based on the current design approach in ACI 318 (19). For biaxial loading directions between 0 and 27°, the error or correction required in uniaxial design to avoid unsafe design goes from 1 to 1.12 ($V_{bi} = 1/\cos(27°)V_{uni}$) for a square (symmetric) column. For loading angles between 27° and 45°, the correction in uniaxial design goes from 1.12 to 1.41 ($V_{bi} = 1/\cos(45°)V_{uni}$). To avoid the angle calculation, alternatively, a strength limit check could be added that indicates if the use of an interaction diagram is required. If $\frac{V_{u,x}}{\varnothing V_{n,x}} \geq 0.5$ and $\frac{V_{u,y}}{\varnothing V_{n,y}} \geq 0.5$ ($V_{u,x}$ and $V_{u,y}$ are the projections along two orthogonal x and y axes of V_u – factored shear force -, respectively, and $V_{n,x}$ and $V_{n,x}$ are the shear strength forces, V_n,along the x and y axes, respectively), the column is in a loading condition similar to a shear force applied with an angle between 27° and 63° (reduction strength factor, $\phi = 1$ in Fig. 6 since actual material properties are used). To keep it simple and avoid step functions, a linear interpolation between the strength limits can be introduced. Thus, the linear interaction diagram defined in ACI 318 (19) is,

$$\frac{V_{u,x}}{\varnothing V_{n,x}} + \frac{V_{u,y}}{\varnothing V_{n,y}} \leq 1.5 \tag{5}$$

If this new ACI 318 (19) approach is applied along with the new shear strength estimation, a trilinear curve is defined for design (red solid line), which is shown in Fig. 6. Such solution, besides of its simplicity, also maintains unaltered the traditional approach of unidirectional shear design for loading cases under an angle of 27° or larger than 63° ($\frac{V_{u,x}}{\varnothing V_{n,x}} < 0.5$ or $\frac{V_{u,y}}{\varnothing V_{n,y}} < 0.5$), such that it presents its largest inaccuracy at the strength limit (or angle limit), that is, requiring an extra 12% shear capacity to be safe, which is considered that can be absorbed by strength reduction factors or material over-strength. The application of the code approach, for biaxial shear strength estimation, leaves 3 cases (due to symmetry 5 points are below the trilinear curve) below the trilinear interaction curve that fall right over the circular interaction curve (out of those 3 cases, 2 of them also fall below the circular interaction curve), which means that the strength is underestimated by about 5% (the case above the circular interaction curve) or 20% (for the cases below the circular interaction curve). For all other cases, the trilinear approach predicts conservative estimates of strength. If the traditional uniaxial shear strength approach is used, besides of the 3 cases that fall below the trilinear curve, other 4 cases are also unconservative with the largest error of about 50% (in the case of 45° loading, it corresponds to the distance from the strength value and the corner at $V_{bi}(x)/V_{uni}(x) = V_{bi}(y)/V_{uni}(y) = 1$). Thus, the ACI 318 (19) approach with the trilinear interaction curve recovers the simplicity of uniaxial shear design when one direction for shear is predominant, and when the biaxial design is required similar conservatism is observed compared to the elliptical interaction curve.

3. Conclusions

This paper summarizes the analysis of experimental data that shows that interaction (circular or elliptical) diagram can correctly predict the response of columns under biaxial shear loading, as well as the implications of providing a one-way (uniaxial) shear strength estimation with the expressions of ACI 318 (14). Besides, the new shear design equations are validated under biaxial loading for both cases: considering one-way or uniaxial shear design and biaxial shear design by means of a trilinear interaction curve incorporated in ACI 318 (19).

The expressions of ACI 318 (14) present different levels of conservatism, indicating that when the simple expression is used the level of conservatism is generally sufficient to avoid the consideration of biaxial loading. However, the use of more refined or accurate expressions, as it is with ACI 318 (19), makes the consideration of biaxial shear for design a need. The new expression for shear strength estimate in ACI 318 (19), which shows an improved accuracy, requires the consideration for biaxial loading to ensure conservatism. The trilinear interaction diagram approach included in ACI 318 (19) for biaxial shear loading provides a reliable method for design.

Declaration of Competing Interest

The authors declare that they have no known competing financial interests or personal relationships that could have appeared to influence the work reported in this paper.

Acknowledgments

This work was developed to support the code modification in ACI 318 (19) under the sub-committee group ACI 318-E. The feedback, opinions and suggestions from the sub-committee group and main ACI 318 group are greatly appreciated. The help from Mr. Viral Patel with the preparation of the code change is also thanked.

Appendix A. Supplementary material

Supplementary data to this article can be found online at https://doi.org/10.1016/j.engstruct.2020.110731.

References

[1] Woodward KA, Jirsa JO. Behavior Classification of Short Reinforced Concrete Columns Subjected to Cyclic Deformations. PMFSEL Report No. 80-2, 1980, University of Texas at Austin.

[2] Priestley MJN, Verma R, Xiao Y. Seismic shear strength of reinforced concrete columns. J Struct Eng 1994;120(8):2310–29.

[3] Maruyama K, Jirsa JO. Shear Behavior of Reinforced Concrete Members under Bidirectional Reversed Lateral Loading. CESRL Report No. 79-1, 1979, The University of Texas at Austin.

[4] Umehara H, Jirsa JO. Shear strength and deterioration of short reinforced concrete columns under cyclic deformations. PMFSEL Report No.82-3, 1982, University of Austin, Texas.

[5] Pham TP, Li B. Seismic behavior of reinforced concrete columns with light transverse reinforcement under different lateral loading directions. ACI Struct J 2013;110(5):833–44.

[6] Joh O, Shibata T. Shear failure of reinforced concrete columns due to biaxial lateral

forces. In: 8th World conference on earthquake engineering; 1984. p. 577–84.
[7] Standard specifications for concrete structures Design. JGC No.15, Japan Society of Civil Engineers, 2007, Tokyo, Japan.
[8] Building code requirements for structural concrete and commentary. (2019). ACI 318-19, American Concrete Institute, Farmington Hills, Mich.
[9] Building code requirements for structural concrete and commentary. (2014). ACI 318-14, American Concrete Institute, Farmington Hills, Mich.
[10] Ramirez H, Jirsa JO. Effect of Axial Load on Shear Behavior of Short RC Columns under Cyclic Lateral Deformations. PMFSEL Report No. 80-1, 1980, University of Texas at Austin.
[11] Arakawa T, Arai Y, Mizoguchi M, Yoshida M. Shear resisting behavior of short reinforced concrete columns under biaxial bending-shear. Trans Japan Concr Inst 1989;11:317–24.
[12] Mizoguchi M, Arakawa T, Arai Y, Yoshida M. Shear resisting behavior of short reinforced concrete columns under biaxial bending-shear and varying axial load. Trans Japan Concr Inst 1990;12:347–54.
[13] Kuchma DA, Wei S, Sanders DH, Belarbi A, Novak LC. Development of the One-Way Shear Design Provisions of ACI 318–19 for Reinforced Concrete. ACI Struct J 2019;116(4):285–95.